Chemical Engineering Science 280 (2023) 119067

Contents lists available at ScienceDirect

Chemical Engineering Science

journal homepage: www.elsevier.com/locate/ces

A new approach for the globally optimal design of gasketed plate heat exchangers with variable properties

André L.M. Nahes [a], André L.H. Costa [a], Miguel J. Bagajewicz [b,c,*]

[a] Institute of Chemistry, Rio de Janeiro State University (UERJ), Rua São Francisco Xavier, 524, Maracanã, Rio de Janeiro, RJ CEP 20550-900, Brazil
[b] School of Chemical, Biological and Materials Engineering, University of Oklahoma, 100 E. Boyd St, T331, Norman, Oklahoma 73019, United States
[c] Federal University of Rio de Janeiro (UFRJ), Escola de Química CT, Bloco E, Ilha do Fundão, CEP 21949-900, Rio de Janeiro, RJ, Brazil

ARTICLE INFO

Keywords:
Design-Optimization
Process Systems Engineering
Heat Exchangers
Set Trimming
Smart Enumeration

ABSTRACT

In this paper, we present two novel advances in the design optimization of gasketed plate exchangers. Our first novelty is the use of an ordinary differential model that represents the heat transfer and pressure drop along the surface of the plate considering the variation of the thermophysical properties (density, heat capacity, viscosity, etc.) with temperature. Previous literature did not address this aspect of the problem or addressed it only partially. We also take into account all pass arrangements. Although there is no novelty in this, it adds to making our model comprehensive. The second novelty is the design optimization method used: Partial Set Trimming and Smart Enumeration. This method guarantees global optimality, it is robust (no convergence issues), and it is fast. A new feature added to the Set Trimming methodology is Proxy Set Trimming. The advantage of Set Trimming followed by Smart Enumeration is that there is no need to discretize the differential equations and build very large models with the resulting large number of variables and algebraic equations, rendering highly non-convex models difficult to solve using MINLP procedures. A comparison of the performance of the proposed procedure with two different metaheuristic methods showed that this approach presents better computational performance.

1. Introduction

Gasketed plate heat exchangers are traditionally used in food, beverages, and pharmaceutical industries (Saunders, 1988; Shah and Sekulic, 2003; Cao, 2010) and as an alternative to shell-and-tube exchangers in chemical process plants. They are viable options for thermal duties at temperatures below 180 °C (compressed asbestos fiber gaskets can operate until 260 °C) and pressures up to 30 bar (Saunders, 1988).

The optimal design problem of gasketed plate heat exchangers was addressed by several authors, which explored three main optimization techniques: metaheuristic methods mathematical programming, and enumeration techniques. The main metaheuristic method employed in the design investigations was genetic algorithms, usually applied to multiobjective optimization problems (Najafi and Najafi, 2010; Saleh et al., 2013; Hajabdollahi et al., 2013; Imran et al., 2017; Shokouhmand and Hasanpour, 2020). The application of mathematical programming to the plate heat exchanger design was explored by Wang and Sundén (2003), using nonlinear programming (NLP), and Martins et al. (2019), using mixed-integer linear programming (MILP). Different alternatives of enumeration techniques were explored by Gut and Pinto, (2004); Picón-Núñez et al., (2010); Zhu and Zhang, (2004), and Mota et al. (2014). A hybrid alternative involving enumeration and mathematical programming, through mixed-integer nonlinear programming (MINLP), was explored by Xu et al. (2022).

Despite some promising results, these design optimization techniques present some important limitations. Metaheuristic methods can travel through different local minima of the problem, but do not guarantee global optimality, and are dependent on the tuning of the algorithm control parameters. Because of the nonlinearity of the heat exchanger model, mathematical programming techniques may present convergence problems and a local minimum solution may be found if a conventional local solver is used. Enumeration techniques are robust, but they may be slow (e.g. exhaustive enumeration). A different alternative for the solution to the design problem, which avoids these problems, was explored by Nahes et al. (2021), using a new optimization alternative method, called Set Trimming. This method handles sets of candidates, instead of individual alternatives, and always attains the global optimum.

Another important aspect of the optimal design problem is the nature of the heat exchanger model employed. Despite the significant advances in plate heat exchanger modeling, the majority of the papers about design optimization employed models based on analytical solutions, particularly, the LMTD and ε-NTU methods. The ε-NTU method was

* Corresponding author.

https://doi.org/10.1016/j.ces.2023.119067
Received 13 February 2023; Received in revised form 19 June 2023; Accepted 2 July 2023
Available online 3 July 2023

Nomenclature

A_{tot}	Total area of the plates (m^2)
C_{cap}	Capital cost ($)
$C_{op,c}$	Yearly operating cost for the cold stream ($/y)
$C_{op,h}$	Yearly operating cost for the hot stream ($/y)
Cp_n	Stream heat capacity in channel n (J/(kg • K))
Cp^{MAX}	Maximum heat capacity (J/(kg • K))
CS	Set of candidates
D_{hyd}	Hydraulic diameter (m)
Dp	Port diameter (m)
f_n	Friction factor in channel n
G_n	Mass flux in channel n (kg/(s • m^2))
h	Convective heat transfer coefficient (W/(m^{2}K))
$\hat{i}$	Interesting rate
k^{MAX}	Maximum thermal conductivity (W/(m • K))
$\widehat{kw}$	Thermal conductivity of the plate material (W/(m • K))
LB	Lower bound
Lp	Projected plate length (m)
Lv	Vertical port distance (m)
Lw	Plate width (m)
mc_n	Mass flow rate in channel n (kg/s)
MTD^{UB}	Upper bound on the mean temperature difference (K)
$\hat{n}$	Project horizon
$\hat{N}_{op}$	Number of operating hours (y)
Npc	Number of passes of cold stream
Nph	Number of passes of hot stream
Ntp	Total number of plates
OF	Objective function
OF^{INC}	Objective function of the incumbent
$\hat{p}_c$	Energy price ($/kWh)
P_n	Stream pressure in channel n (Pa)
Q	Heat load (W)
Q^{UB}_{spec}	Upper bound on the evaluated heat load (W)
$\hat{Q}_{esp}$	Specified minimum heat load (W)
$q_{n,n-1}$	Thermal flux between the channels n and $n-1$ (W/m^2)
$\hat{r}$	Annualizing factor (y^{-1})
Rf	Foulign factor (m^{2}K/W)
$\widehat{Tc_i}$	Inlet temperature of the cold stream (°C)
$\widehat{Tc_o}$	Outlet temperature of the cold stream (°C)
$\widehat{Th_i}$	Inlet temperature of the hot stream (°C)
$\widehat{Th_o}$	Outlet temperature of the hot stream (°C)
$\hat{t}$	Plate thickness (m)
TAC	Total annualized cost ($/y)
T_n	Stream temperature in channel n (°C)
U^{UB}	Upper bound on the overall heat transfer coefficient (W/(m^{2}K))
v	flow velocity in the channels (m/s)
v^{LB}	Lower bound of the flow velocity (m/s)
v^{UB}	Upper bound of the flow velocity (m/s)
$\hat{v}_{max}$	Upper of the flow velocity bound (m/s)
$\hat{v}_{min}$	Lower of the flow velocity bound (m/s)
y	Spatial coordinate (m)

Greek Symbols

β	Chevron angle (deg)
$\hat{\Phi}$	Surface enlargmenet factor
ρ_n	Stream density in channel n (kg/m^3)
ρ^{MAX}	Maximum density (kg/m^3)
ρ^{MIN}	Minimum density (kg/m^3)
μ	Viscosity (Pa·s)
μ^{MIN}	Minimum viscosity (Pa·s)
$\hat{\eta}$	Pump efficiency
ΔPt	Total pressure drop (Pa)
ΔPt^{LB}	Lower bound on the pressure drop (Pa)
$\widehat{\Delta P}_{disp}$	Available pressure drop (Pa)

employed by Hajabdollahi et al. (2016), Imran et al. (2017), and Raja et al. (2018). The LMTD method was employed in optimization problems by Guo-Yan et al., (2008); Nahes et al., (2021); Picón-Núñez et al., (2010); Zhu and Zhang, (2004), and Xu et al. (2022). The models employed by these papers ignored the physical properties variation with temperature and also did not consider the effects associated with the end plates. Other papers solved the design optimization problem using models based on the analytical solution of the linear system of ordinary differential equations associated with the energy balances. These models are more rigorous than the LMTD and ε-NTU methods, thus they can predict end plate effects, but they still ignore the variation of the physical properties with temperature (Mota et al., 2014; Shokouhmand and Hasanpour, 2020).

The utilization of models based on analytical solutions can attain satisfactory accuracy in many problems, but they may lead to significant deviations in design problems that involve streams with large physical properties variations (e.g. engine oil). According to our knowledge, the solution of the optimal design problem using models associated with computational routines for the numerical integration of the corresponding system of differential equations was only addressed by Gut and Pinto (2004), but with limitations (the pressure drop evaluation is based on algebraic relations that were derived considering uniform physical properties). Alternatively, surrogate models were also tested for the design optimization of gasketed plate heat exchangers by Saleh et al. (2013).

The wider utilization of analytical models for design optimization can be explained by the difference in the computational effort involved. The most common analytical models are represented by a few algebraic equations, and more sophisticated models are needed for the representation of the variation of the physical properties, depending on numerical discretization procedures.

We now address the difficulties of models that take into account the variation of properties with temperature. Most design optimization models are presented as mixed integer nonlinear optimization models, which can be represented as follows

$$\text{Min}\, f(x) \tag{1}$$

s.t.

$$g(x, y, z) \le 0 \tag{2}$$

$$h(x, z, y) = 0 \tag{3}$$

$$x, z \in \Re^n \tag{4}$$

$$y \in \{0, 1\}^m \tag{5}$$

Usually, all functions are linear in the binary variables, or reformulations exist that can linearize these functions rigorously, many times with the addition of some new continuous variables. However, many equipment are modeled by a set of differential equations. This leads to mixed integer nonlinear differential–algebraic optimization models, as follows:

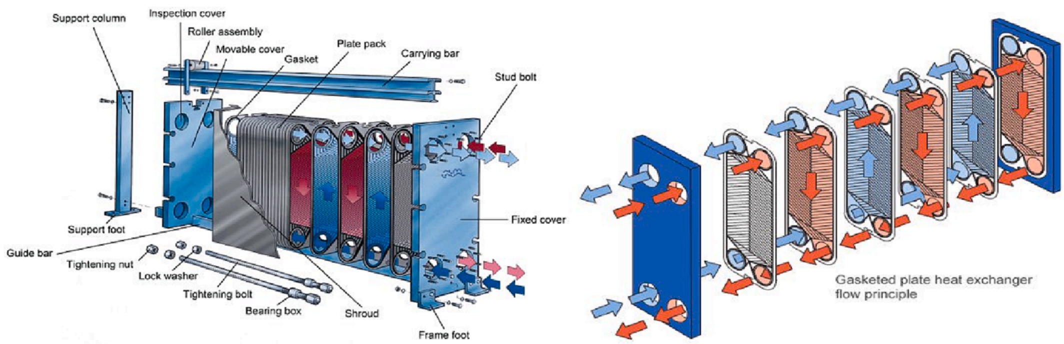

Fig. 1. Gasketed plate exchanger (Courtesy of Alfa Laval).

$$\text{Min} f(x) \tag{6}$$

s.t.

$$g(x, y, z) \leq 0 \tag{7}$$

$$h(x, z, y) = 0 \tag{8}$$

$$\frac{dx}{dz} = f(x, z, y) \tag{9}$$

$$x, z \in \Re^n \tag{10}$$

$$y \in \{0.1\}^m \tag{11}$$

In most cases, the differential equations represented by Eq. (9) are discretized, which allows the reformulation of the problem to a mixed integer nonlinear optimization model (Eqs. (1)–(5). The price one pays for this discretization is large. Discretization requires a lot of equations, crippling the ability of the optimization methods that use mathematical programming (we leave aside metaheuristics for the reasons stated above) to find initial feasible solutions and/or converge in a reasonable time. In our case, consider a plate exchanger with 101 plates associated with 100 channels, with a unidimensional energy balance equation in differential form, discretized using 20 points. This means that 2000 equations and 2000 variables are added. In addition, if the model needs to differentiate among different pass arrangements several binaries are needed to determine the direction of flow in each channel. These are 2000 binaries. We have not tried to build such a large model.

The literature also considers a variety of models with different pass arrangements, but a comprehensive optimization model considering all the possible arrangements of passes has not fully been fully addressed considering the variation of the physical properties for the energy and mechanical energy balances.

In this article, we present a methodology for gasketed plate exchanger design using a more rigorous mathematical model, which can describe the variation of the physical properties with temperature and end plate effects. We also use a model that takes into account different pass arrangements, making it comprehensive. Unlike the case of models that are solved using MINLP approaches, where several branching binary constraints are used, the addition of these options does not have an impact on our solution procedure, other than some marginal increase in computational time. Despite the higher model complexity, the optimization algorithm is computationally efficient, keeping the solution time limited to acceptable values. This task is solved using Partial Set Trimming followed by Smart Enumeration (Costa and Bagajewicz, 2019). Partial Set Trimming is used as a preprocessing step to reduce the number of candidates. Smart Enumeration identifies the solution through the simulation of a small fraction of the search space of solution candidates. This procedure always finds the global optimum solution, does not involve any parameter tuning, and does not present convergence problems (assuming that the simulation algorithm is robust).

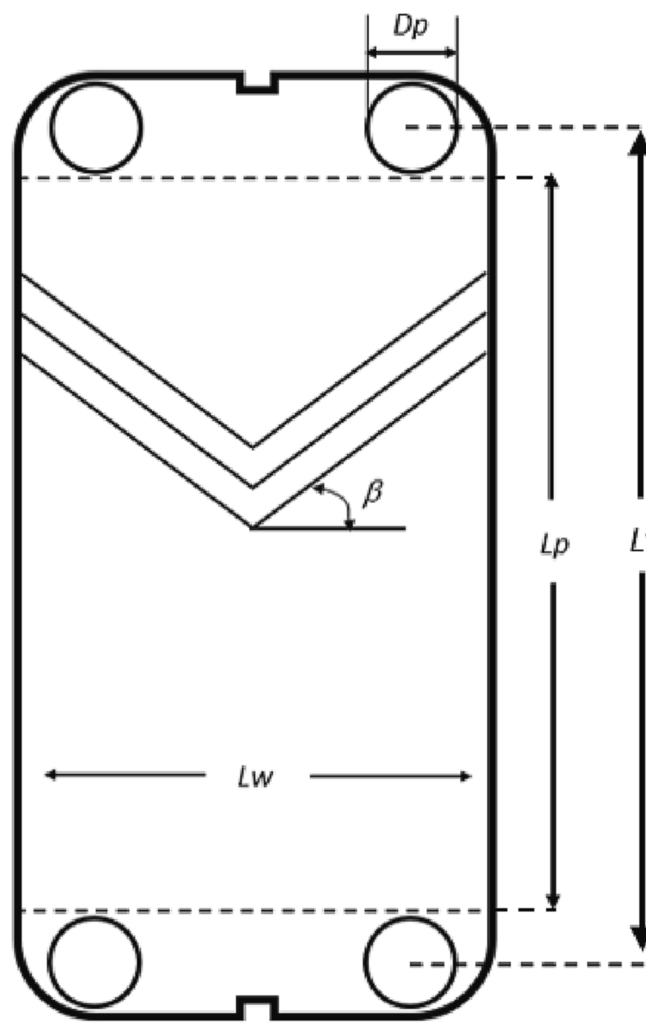

Fig. 2. Plate dimensions.

The paper is organized as follows: We first summarize the heat transfer and pressure drop equations of the heat exchanger model, which have been presented in detail by Nahes et al. (2022). Next, we discuss the design optimization procedure, including the independent variables and the objective function. Following, we summarize the two components of the design optimization procedure, namely, Partial Set Trimming and Smart Enumeration. We then present the results, including a comparison of the effectiveness of our methodology with the use of metaheuristics and the effect of assuming uniform properties on the design when the properties vary significantly with temperature.

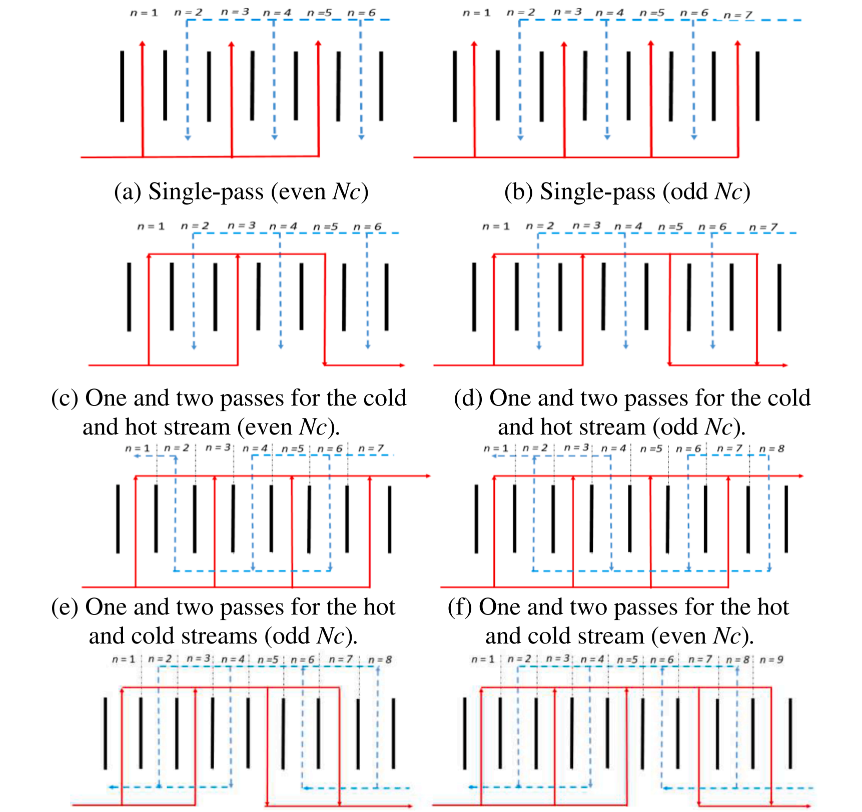

(a) Single-pass (even Nc) (b) Single-pass (odd Nc)

(c) One and two passes for the cold and hot stream (even Nc). (d) One and two passes for the cold and hot stream (odd Nc).

(e) One and two passes for the hot and cold streams (odd Nc). (f) One and two passes for the hot and cold stream (even Nc).

(g) Two passes for both streams (even Nc). (h) Two passes for both streams (odd Nc).

Fig. 3. Plate heat exchangers arrangements.

Finally, we make concluding remarks.

2. Gasketed-plate heat exchanger model

The structure of a gasketed plate heat exchanger is illustrated in Fig. 1. The heat exchanger is composed of a set of parallel corrugated plates. A channel is formed between each pair of plates, where the hot and cold streams flow through these channels, and heat is transferred across the plates. The plates have gaskets that prevent the leak of the streams from the heat exchanger.

The plates are corrugated, which promotes flow turbulence and enhances the heat transfer coefficient, as well as improves the rigidity of the plates (Shah and Sekulic, 2003). The main dimensions of the plate are shown in Fig. 2, where Lw is the plate width inside gaskets, Lp is the projected plate length, Lv is the vertical port distance, Dp is the port diameter, and β is the Chevron angle (Kakac and Liu, 2002).

The proposed optimization approach is versatile and can be employed using any heat exchanger model. Particularly in this paper, the design problem is solved using the model proposed by Nahes et al. (2022). This model corresponds to a set of differential equations representing the energy and mechanical energy balances. An important aspect of this model is its generalized nature, where any heat exchanger configuration of pass arrangements (Fig. 3) can be represented through the proper selection of a given set of input parameters.

The energy balance in a channel n is given by (axial diffusion and viscous dissipation are dismissed):

$$\frac{dT_n}{dy} = -pn_n \frac{Lw\widehat{\Phi}}{mc_n Cp_n}\left(q_{n,n-1} + q_{n,n+1}\right) \quad (12)$$

where T_n is the stream temperature in the channel n, Cp_n is the stream heat capacity in the channel n, y is the spatial coordinate along with the plate height, $\widehat{\Phi}$ is the surface enlargement factor, mc_n is the mass flow rate in the channel n (which is affected by the number of passes), $q_{n,n-1}$ is the thermal flux between the channels n and n-1, and $q_{n,n+1}$ is the thermal flux between the channels n and $n + 1$. In turn the heat flux transferred across the plates is given by the following equations:

$$q_{n,n-1} = U_{n,n-1}(T_n - T_{n-1}) = \frac{(T_n - T_{n-1})}{\frac{1}{h_{n-1}} + Rf_{n-1} + \frac{\hat{t}}{\widehat{kw}} + Rf_n + \frac{1}{h_n}} \quad (13)$$

$$q_{n,n+1} = U_{n,n+1}(T_n - T_{n+1}) = \frac{(T_n - T_{n+1})}{\frac{1}{h_{n+1}} + Rf_{n+1} + \frac{\hat{t}}{\widehat{kw}} + Rf_n + \frac{1}{h_n}} \quad (14)$$

where U is the overall heat transfer coefficient, h is the convective heat transfer coefficient, Rf is the fouling factor, $\hat{t}$ is the plate thickness, and $\widehat{kw}$ is the thermal conductivity of the plate material. The convective heat transfer coefficients are calculated using proper correlations (Kakaç and Liu, 2002).

The hydraulic model addresses the pressure drop associated with friction losses. The pressure drop in a channel n can be evaluated using the Darcy–Weisbach equation, represented by the following differential equation:

$$\frac{dP_n}{dy} = \frac{f_n G_n^2}{2D_{hyd}\rho_n} \quad (15)$$

where f_n is the friction factor in the channel n, which depends on the Reynolds number, P_n is the stream pressure in the channel n, G_n is the mass flux in the channel n, D_{hyd} is the hydraulic diameter of the channels, and ρ_n is the stream density in channel n.

The heat exchanger model solution is obtained through the resolution of the system of algebraic equations obtained from the discretization of Eqs. (12)–(15). Additional details of this model have been discussed and used for simulations by Nahes et al. (2022).

Two key issues are particularly addressed in the proposed model, which eliminates important limitations present in the literature: (a) The proposed model consists of a set of equations in a single generalized structure addressing any arrangement of passes and (b) the variation of the physical properties with temperature is included in the model explicitly.

3. Design optimization

The design optimization problem addresses gasketed plate heat exchangers with Chevron-type plates for the heating/cooling of streams without phase change. The design variables that represent each solution candidate are:

- Total number of plates (*Ntp*),
- Plate size (defined by the plate length, *Lp*, plate width, *Lw*, and port diameter, *Dp*),
- Chevron angle (β),
- Number of passes of each stream (*Nph* and Npc, respectively).

Due to the commercial availability and/or physical nature of the design variables, their values must be selected among a set of discrete options. The plate thickness $(\hat{t})$, the surface enlargement factor $(\hat{\Phi})$, and the mean channel spacing are fixed parameters associated with the plate type and are not included in the optimization.

Two design formulations are explored. The first corresponds to the minimization of the total area of the plates, which is directly related to the equipment capital cost:

$$\min A_{tot} = Ntp\ \hat{\Phi}\ Lw\ Lp \tag{16}$$

The performance constraints consist of the bounds on flow velocities, available pressure drops, and the minimum heat load required to fulfill the thermal task, as follows:

$$\hat{v}_{min} \leq v \leq \hat{v}_{max} \tag{17}$$

$$\Delta Pt \leq \widehat{\Delta P}_{disp} \tag{18}$$

$$Q \geq \hat{Q}_{spec} \tag{19}$$

where *v* is the flow velocity in the channels between the plates, $\hat{v}_{min}$ and $\hat{v}_{max}$ are the upper and lower flow velocity bounds, ΔPt is the total pressure drop, $\widehat{\Delta P}_{disp}$ is the available pressure drop, Q and $\hat{Q}_{esp}$ are the heat exchanger heat load and the specified minimum heat load of the design task, respectively. The specified minimum heat load can consider any design margin established by the practitioner, e.g. typically 10% (Towler and Sinnot, 2008). The constraints represented in Eqs. (17) and (18) must be applied to both streams.

Alternatively, the design optimization can be formulated as the minimization of the total annualized cost, including capital and operating costs. In this case, the constraint related to the pressure drop bounds in Eq. (18) is eliminated and the objective function displayed in Equation (16) is substituted by:

$$\min\ TAC = \hat{r}C_{cap} + C_{op,h} + C_{op,c} \tag{20}$$

where *TAC* is the total annualized cost, C_{cap} is the capital cost, $C_{op,h}$ and $C_{op,c}$ are the yearly operating costs for the hot and cold streams, and $\hat{r}$ is the annualizing factor. The expression of the annualizing factor is:

$$\hat{r} = \frac{\hat{i}(1+\hat{r})^{\hat{n}}}{(1+\hat{r})^{\hat{n}} - 1} \tag{21}$$

where $\hat{i}$ is the interesting rate and $\hat{n}$ is the project horizon in years.

The capital cost is evaluated by:

$$C_{cap} = \hat{a}_c A_{tot}^{\hat{b}_c} \tag{22}$$

where $\hat{a}_c$ and $\hat{b}_c$ are model parameters of the cost correlation. The expression for the evaluation of the energy consumption for each stream is given by:

$$C_{op} = \hat{N}_{op}\frac{\hat{p}_c}{10^3}\left(\Delta P\frac{\hat{m}}{\hat{\eta}\rho}\right) \tag{23}$$

where $\hat{p}_c$ is the energy price, $\hat{m}$ is the mass flow rate (hot or cold), $\hat{\eta}$ is the pump efficiency, and $\hat{N}_{op}$ is the number of operating hours per year.

4. Design optimization procedure

The optimization procedure encompasses two steps: Partial Set Trimming followed by Smart Enumeration. The search space is represented by a combinatorial representation of the available values of the different optimization variables. Each solution candidate corresponds to a given combination of all the design variables. Thus, given a selected candidate, its performance can be obtained through the solution of the mathematical model, as well as the evaluation of the corresponding value of the objective function.

4.1. Partial set trimming

Set Trimming is an extension and generalization of the screening step in the optimization procedure developed by Gut and Pinto (2004) for the design of gasketed plate heat exchangers, which is related to a procedure employed by Daichendt and Grossmann (1994) for heat exchanger network synthesis. The proposition of Set Trimming as a complete and autonomous optimization technique for equipment design was presented by Costa and Bagajewicz (2019).

The Set Trimming procedure consists of the successive application of the problem inequality constraints to sets of candidates to eliminate infeasible options. Each trimming step can reduce the number of solution candidates, therefore the sequence of trimmings yields a sequence of gradually smaller sets of solution candidates, which allows a reduction of the computational effort. We emphasize that Set Trimming operates through set manipulation techniques instead of analyzing candidates one by one.

If all constraints are applied, then the resultant set corresponds to the feasible region and the global optimum can be identified through a sorting procedure based on the values of the objective function of the remaining solution candidates. This procedure is called Complete Set Trimming and was applied successfully to the design optimization of gasketed plate heat exchangers, based on analytical models, by Nahes et al. (2021).

However, this technique cannot be fully employed in more complex methods, when the evaluation of the constraints cannot be applied to entire sets, but it demands the iterative solution of individual solution candidates, as the model present above (the design constraints given by Eqs. (12)–(15) cannot be evaluated without the mathematical model solution).

Aiming at circumventing this obstacle, Partial Set Trimming is applied here. Partial Set Trimming involves the direct utilization of the simpler constraints and/or the utilization of constraint relaxations of the more complex ones. These original simpler constraints and the relaxations of the complex constraints can be evaluated using specialized routines for set manipulations, similar to the conventional Set Trimming. The utilization of the relaxations for eliminating infeasible candidates is called Proxy Set Trimming.

Proxy Set Trimming can reduce the number of candidates, but it cannot eliminate all infeasible solutions. Therefore, at the end of the process, the resultant set contains all the feasible candidates together with a certain number of infeasible ones. The identification of the global

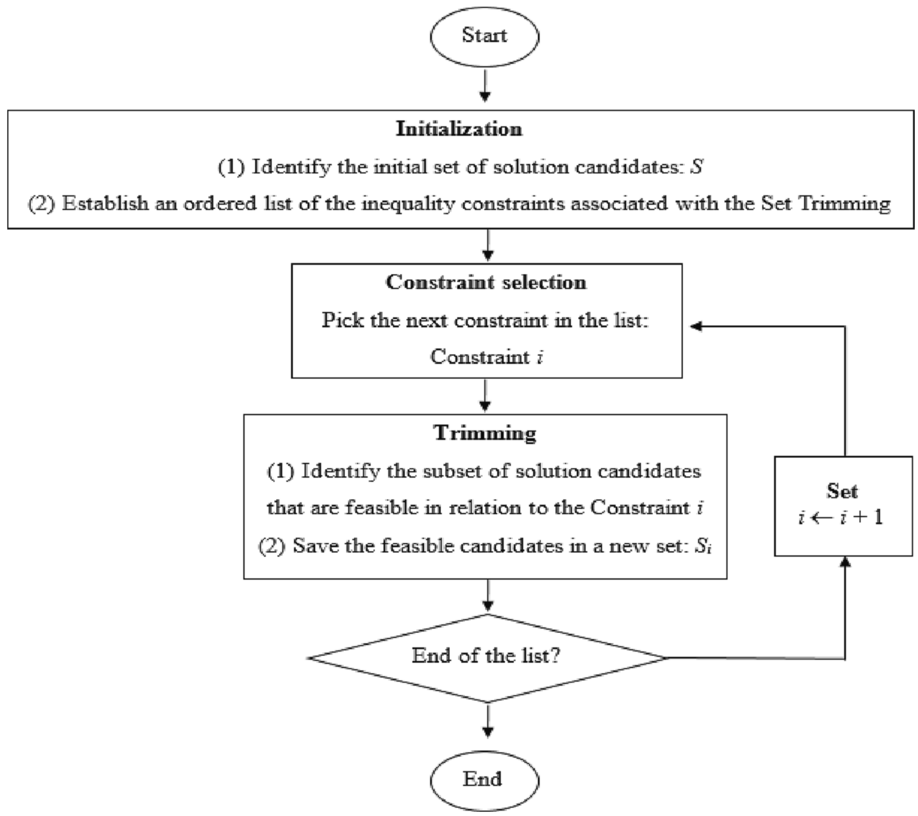

Fig. 4. Set Trimming procedure.

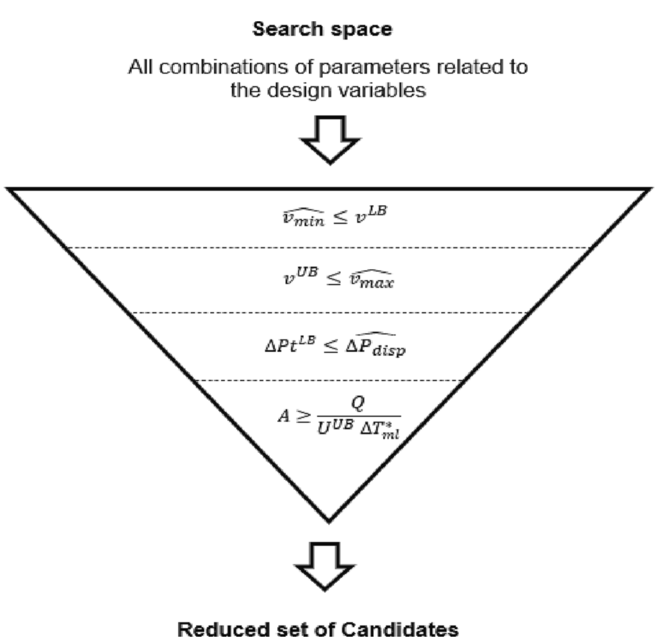

Fig. 5. Set Trimming sequence in design optimization.

optimum within this reduced set is obtained through a subsequent enumeration procedure, described in the next section.

The constraints employed in the Proxy Set Trimming are related to the original constraints of Eqs. (17)–(19), are:

$$\widehat{v_{min}} \leq v^{UB} \tag{24}$$

$$\widehat{v_{max}} \geq v^{LB} \tag{25}$$

$$\widehat{\Delta P_{disp}} \geq \Delta Pt^{LB} \tag{26}$$

$$Q^{UB}_{spec} \geq \widehat{Q}_{spec} \tag{27}$$

where v^{LB} and v^{UB} are, respectively, the lower and upper bounds on the flow velocity, ΔPt^{LB} is a lower bound on the pressure drop and Q^{UB}_{spec} is an upper bound on the evaluated heat load. This set of relaxations is easily performed for entire sets of candidates, exploring the modern routines for handling large sets of data (e.g. arrays in NumPy module of Python, vectorization resources available in Matlab or Scilab, etc.).

Fig. 4 presents a representation of the Set Trimming step. The order of the constraints employed in the Set Trimming is Eq. (24) → Eq. (25) → Eq. (26) → Eq. (27), where the constraints in Eqs. (24)–(26) are applied to both streams. Fig. 5 illustrates the reduction of the number of candidates along the algorithm advance.

The details of the construction of the bounds v^{LB}, v^{UB}, ΔPt^{LB} and Q^{UB}_{spec} are shown next.

4.1.1. *Bounds associated with the Proxy Set Trimming*

The bounds employed in the Proxy Set Trimming for velocity and pressure drop are based on the assumption of uniform physical properties, which yields simple algebraic relations that can be used for trimming sets of candidates. The values of the uniform physical properties are selected in order to provide the desired upper/lower bounds (e.g. a reduction of the viscosity reduces the pressure drop, therefore, the lowest viscosity value is associated with a pressure drop lower bound).

The lower bound on the pressure drop, associated with the constraint in Eq. (26) is given by:

$$\Delta Pt^{LB} = \left(\frac{\Delta Pc}{\Delta z}\right)^{LB} L + 1.4Np\frac{Gp^2}{2\rho^{MAX}} \tag{28}$$

where $\left(\frac{\Delta Pc}{\Delta z}\right)^{LB}$ is a lower bound on the pressure gradient in the channels,

Table 1
Physical properties condition evaluation.

Property	Physical properties evaluation to the Proxy Set Trimming
μ^{MIN}	Inlet hot stream temperature
ρ^{MIN}	Inlet hot stream temperature
ρ^{MAX}	Inlet cold stream temperature
k^{MAX}	Inlet cold stream temperature
Cp^{MAX}	Inlet hot stream temperature

evaluated by the RHS of Eq. (15), considering the following uniform conditions of the stream: minimum viscosity (μ^{MIN}) and maximum density (ρ^{MAX}). The second term in the RHS of Eq. (28) corresponds to a lower bound on the pressure drop in the flow inside the port ducts (Kakaç and Liu, 2002).

In turn, the velocity bounds associated with the constraints in Eqs. (24)–(25) are given by:

$$v^{UB} = \frac{\widehat{m}/Ncp}{\rho^{MIN}\widehat{b}Lw} \tag{29}$$

$$v^{LB} = \frac{\widehat{m}/Ncp}{\rho^{MAX}\widehat{b}Lw} \tag{30}$$

Finally, the upper bound on the heat load, associated with the constraint of Eq. (27), can be evaluated through an analytical model based on the LMTD method, as follows:

$$Q_{spec}^{UB} = U^{UB}\ A\ MTD^{UB} \tag{31}$$

where U^{UB} and MTD^{UB} correspond to the upper bounds on the overall heat transfer coefficient and mean temperature difference, respectively. The evaluation of U^{UB} is based on the evaluation of the convective heat transfer coefficient of each stream using the same correlations of the original model at the following conditions: minimum viscosity (μ^{MIN}), maximum thermal conductivity (k^{MAX}), and maximum heat capacity (Cp^{MAX}). These limits were defined according to an analysis of the mathematical expressions of the convective heat transfer correlations and are coherent with the expected physical behavior, i.e. the heat transfer coefficient increases for a stream with lower viscosity, higher thermal conductivity and higher heat capacity.

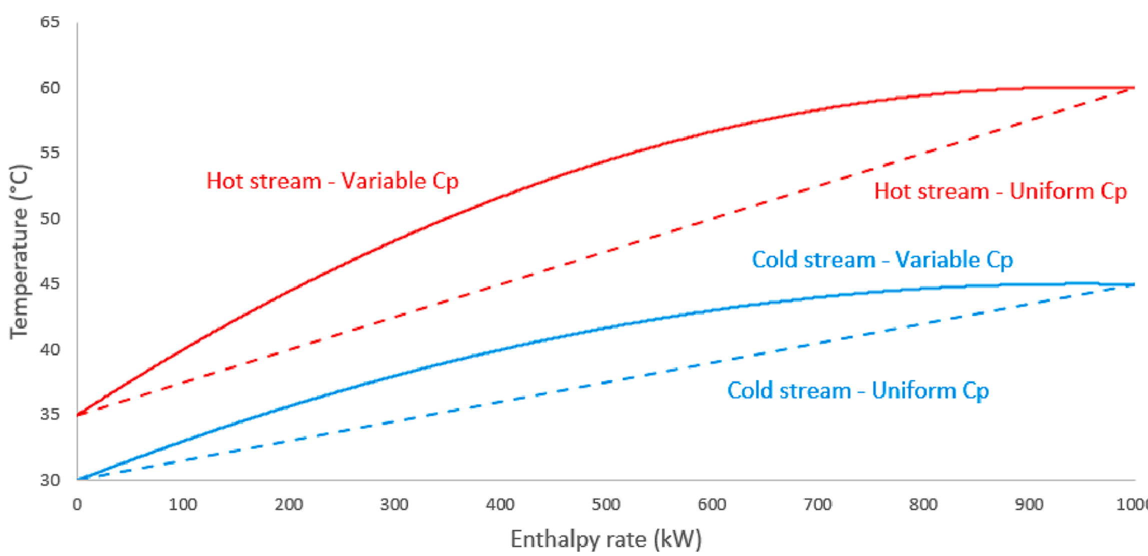

Fig. 6. Stream's temperature vs enthalpy profiles inside an exchanger.

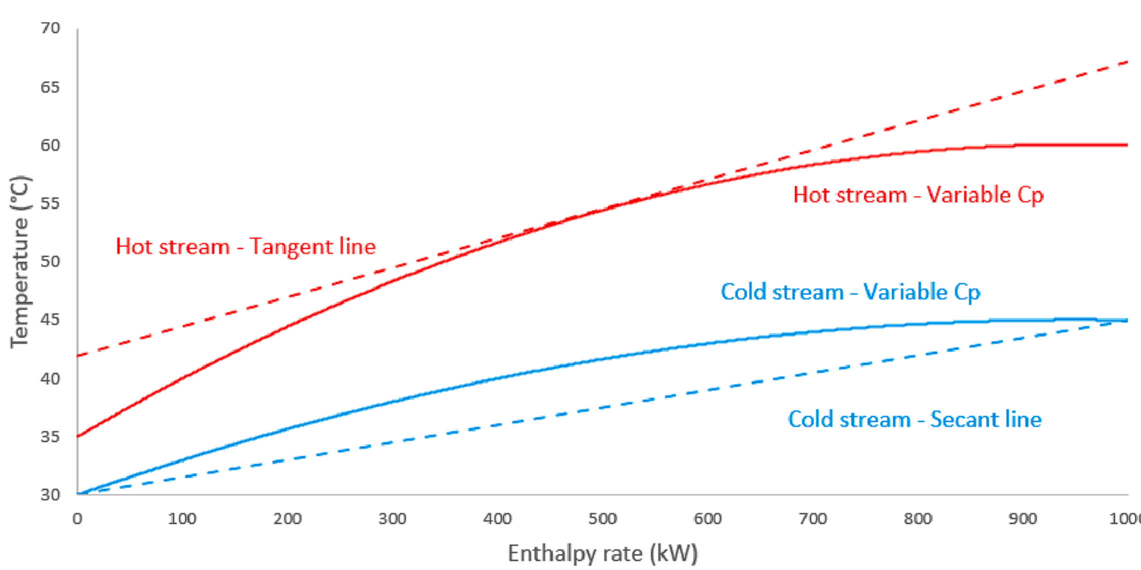

Fig. 7. *LMTD* method upper bound.

If the dependence of the physical properties on temperature is monotonic, the limit values of the physical properties discussed above are easily obtained using the inlet or outlet conditions of the hot and cold streams. For example, the corresponding property limits for the engine oil stream addressed in the design examples of the Results section are depicted in Table 1. Otherwise, it is necessary to create a temperature mesh between the inlet and outlet temperature and evaluate the physical properties at each point of the mesh, and select the desired one (maximum or minimum value).

The logarithmic mean temperature difference of the countercurrent configuration is an upper bound of the MTD, according to the LMTD method (Shah and Sekulic, 2003). However, this result is obtained assuming a constant value of the heat capacity, which is associated with a linear relationship between temperature and enthalpy (T-H). Since the original problem deals with heat capacities that depend on the temperature, the T-H relations are not linear and the MTD between the hot and cold stream predicted by the LMTD method may be underestimated. For example, Fig. 6 shows an example of rigorous T-H profiles of the hot and cold streams and the corresponding linear profiles associated with the LMTD method. It is possible to observe that the LMTD does not provide a rigorous upper bound of the MTD, because the heating curve of the hot stream is above the linear relation.

Thus, it is necessary to establish an adequate upper bound of the *MTD*. The highest possible value of the MTD is the difference between the inlet temperatures, but this value is too large and reduces the Set Trimming elimination. Thus, a lower one can be obtained considering straight lines that can be determined, as follows.

Let $T_h = f_h(H)$ and $T_c = f_c(H)$ and let $(a + b\,H)$ and $(c + d\,H)$, be the desired bounding straight lines, where *a, b, c,* and *d*, are the unknown coefficients sought after. The best LMTD approximation can be obtained by solving the following problem (see Fig. 7):

$$Min\Delta T^*_{ml} = \frac{\left(T^*_{h,in} - T^*_{c,out}\right) - \left(T^*_{h,out} - T^*_{c,in}\right)}{\ln\left[\frac{\left(T^*_{h,in} - T^*_{c,out}\right)}{\left(T^*_{h,out} - T^*_{c,in}\right)}\right]} \tag{32}$$

s.t.

$$a + bH \geq f_h(H)\ H \in (0, \widehat{Q}) \tag{33}$$

$$c + dH \leq f_c(H)\ H \in (0, \widehat{Q}) \tag{34}$$

$$T^*_{h,in} = a + b\,\widehat{Q}\ H \in (0, \widehat{Q}) \tag{35}$$

$$T^*_{h,out} = a\ H \in (0, \widehat{Q}) \tag{36}$$

$$T^*_{c,out} = c + d\,\widehat{Q}\ H \in (0, \widehat{Q}) \tag{37}$$

$$T^*_{c,in} = c\ \ H \in (0, \widehat{Q}) \tag{38}$$

Usually, the variation of the slope of the T-H curves in the operating range of liquid streams in gasketed plate heat exchangers is not very large, therefore, instead of solving the optimization problem represented by Eqs. (32)–(38), an alternative approach is to evaluate the upper bound on the MTD using the inlet and outlet temperatures of the cold stream (associated with the corresponding straight line in the T-H diagram) and hot stream temperatures associated with the enthalpy variation along any tangent line (e.g. the tangent at the middle point). This approach is valid when the heat capacity increases with temperature, which is the usual behavior.

4.2. Smart enumeration

After the Partial Set Trimming step, all infeasible candidates are not eliminated, and the surviving set is composed of feasible and infeasible ones. Therefore, an additional step is required to identify the feasible option with the lowest value of the objective function in the reduced set of candidates obtained by the Set Trimming procedure. Instead of solving the mathematical model of all remaining candidates (i.e. an exhaustive enumeration), the proposed procedure involves the evaluation of only a fraction of the current solution candidates. This procedure is called "Smart Enumeration" and was outlined by Costa and Bagajewicz (2019).

Initially, the procedure evaluates a lower bound of the objective function of each remaining candidate and organizes the candidates according to an ascending order of their lower bounds. This lower bound must be easily evaluated, consuming a small computational time and the gap between its value and the rigorous solution should be low. Then, the candidates are simulated, one by one, starting from the smallest lower bound. If a candidate is feasible, its objective function is evaluated and compared with the corresponding incumbent. Then, if a better solution is found, the incumbent is updated. The procedure continues until the current candidate's lower bound becomes larger than the objective function of the incumbent. This guarantees that the global optimum was found.

The complete algorithm for Smart Enumeration is described below:

<u>Initialization:</u>

- Identify the reduced set of candidates from the Partial Set Trimming.
- Evaluate the lower bound of the objective function (LB) for all candidates.
- Initialize the objective function (OF) of the incumbent, $OF^{INC} = \infty$.
- Arrange the set of candidates (CS) in ascending order of the LB:

$$CS = \{LB_1, LB_2, \cdots, LB_i, \cdots\}, \text{such that}, LB_{i+1} \geq LB_i$$

- Set $i = 1$

<u>Step 1</u>: If $CS = \varnothing$, then stop, the solution corresponds to the incumbent; if no incumbent was updated, then the problem has no feasible candidates.

<u>Step 2</u>: Pick the next candidate, i, in the set CS, associated with a lower bound.LB_i

<u>Step 3</u>: If $OF^{INC} \leq LB_i$, then stop, the solution is the incumbent.

<u>Step 4</u>: Solve the mathematical model of Candidate i for evaluation of the problem constraints of this candidate.

<u>Step 5</u>: If the Candidate i is infeasible, then go to Step 7, else, evaluate the objective function of this candidate,.OF_i

<u>Step 6</u>: If $OF_i < OF^{INC}$, then update the incumbent,.$OF^{INC} \leftarrow OF_i$

<u>Step 7</u>: Eliminate the tested candidate from the active set of candidates ($CS \leftarrow CS \backslash \{LB_i\}$).

<u>Step 8</u>: Set $i \leftarrow i+1$ and go to Step 1.

The TAC objective function is composed of the capital and operating costs (Eq. (20)). The capital costs can be easily evaluated through the heat transfer area of the candidate, but the operating costs depend on the pressure drops, which are not known before the mathematical model solution. In this case, Eq. (28) can be used to generate the TAC lower bound.

The design problem represented by the area minimization is simpler because the objective function of a candidate can be evaluated without the simulation results. In this case, it is not necessary to use an objective function lower bound and an incumbent analysis. The global optimum is identified when the first feasible candidate is found in an ordered set of candidates, as follows.

<u>Initialization:</u>

- Identify the initial set of candidates from the Partial Set Trimming
- Evaluate the objective function (OF) for all the candidates.
- Arrange the set of candidates (CS) in ascending order of OF:

Table 2
Values of the discrete design variables.

Variable	Value
Total number of plates	10, 11, 12, …, 800
Plate size alternative (Table 9)	1, 2, 3, 4, 5
Chevron angle (deg)	30, 45, 50, 60, 65
Hot/cold stream number of passes	1 and 2

Table 3
Dimensions of the plate size alternatives.

Alternative	Plate length Lp (m)	Plate width Lw (m)	Port diameter Dp (m)
1	0.743	0.845	0.3
2	0.978	0.812	0.288
3	1.281	1.200	0.4
4	1.50	1.22	0.35
5	1.835	0.945	0.3

Table 4
Design examples specifications.

		Examples				
Stream	Parameter	1	2	3	4	5
Hot	$\widehat{Th}_i$(°C)	150.00	150.00	160.00	160.00	160.00
	$\widehat{Th}_o$(°C)	130.00	122.00	120.00	143.80	120.00
	$\widehat{mh}$(kg/s)	50	70	25	70	45
	$\Delta\widehat{Ph}_{disp}$ (bar)*	1.0	0.7	0.6	2.0	1.0
Cold	$\widehat{Tc}_i$(°C)	32.00	50.00	62.00	22.00	40.00
	$\widehat{Tc}_o$(°C)	58.75	87.2	106.44	40.00	91.88
	$\widehat{mc}$(kg/s)	45	60	25	80	40
	$\Delta\widehat{Pc}_{disp}$ (bar)*	1.0	0.7	0.6	2.0	1.0

*TAC minimization problems are not limited by the allowable pressure drop.

$$CS = \{OF_1, OF_2, \cdots, OF_i, \cdots\}, \text{such that}, OF_{i+1} \geq OF_i$$

- Set $i = 1$

Step 1: Pick the next candidate, *i*, in the set.*CS*
Step 2: Solve the mathematical model of Candidate *i* for evaluation of the problem constraints of this candidate.
Step 3: If the Candidate *i* is feasible, then stop (the solution is the current candidate), else, Set $i \leftarrow i+1$ and go to Step 1.

5. Results

This paper explores three sets of results. First, we present the optimization results of five examples of plate heat exchanger design problems. Second, we compare the performance of the proposed methodology with two important metaheuristic methods: Genetic Algorithms (Goldberg, 1989) and Particle Swarm Optimization (Kennedy and Eberhart, 1995). Finally, we illustrate the effect of assuming uniform physical properties in the optimal design.

5.1. Plate heat exchanger design optimization

The search space is presented in Tables 2 and 3. All of the plates correspond to a Chevron type, with dimensions typical of industrial models (C. J. Mulanix Company, Inc., 2022). This search space corresponds to 79,000 different candidates, generated through the combination of all possible values of the design variables.

The material of the plates has a thickness and thermal conductivity equal to 0.8 mm and 16.2 W/(m·K), respectively. The enlargement factor associated with the corrugation is 1.15 and the mean channel spacing is 3 mm.

Table 5
Optimization results.

	Optimal result for Area minimization			Optimal result for TAC minimization		
Example	Area (m^2)	TAC ($/y)	Elapsed time (s)	Area (m^2)	TAC ($/y)	Elapsed time (s)
1	91	21,172	93	146	10,782	385
2	199	19,680	323	381	17,149	1747
3	136	9,927	140	143	8,364	261
4	122	52,940	124	242	25,250	994
5	200	17,755	398	317	14,816	1019

Table 6
Global optimum solution details.

	Example	Ntp	Plate	Nph	Npc	β
Area minimization	1	126	1	2	1	60
	2	218	2	1	1	45
	3	77	3	1	1	30
	4	169	1	2	1	60
	5	113	3	1	1	45
TAC minimization	1	202	1	1	1	65
	2	181	4	1	1	65
	3	81	3	1	1	45
	4	340	1	1	1	60
	5	159	5	1	1	65

The hot and cold streams correspond to engine oil, which presents a considerable variation in the viscosity with temperature. The physical properties of the streams are calculated in the simulation using mathematical functions fitted to the set of data in different temperatures present in Incropera and DeWitt (2007) (see Nahes et al. 2022).

The computational codes of the enumeration algorithms were written in Python, employing the module NumPy for fast array manipulations and the module SciPy for handling sparse matrices. The simulations were carried out through a discretization grid of the differential equations containing 25 points. The optimizations were run using a personal computer with a processor i7-8565U 1.8 GHz and 8 GB RAM.

The data from the five design examples investigated are presented in Table 4. In addition, the flow velocity must be within 0.2 and 0.9 m/s and the fouling factor of the cold and hot streams are 0.0002 m$^{2\circ}$C/W and 0.0004 m$^{2\circ}$C/W, respectively. For the TAC minimization, the values of the parameters employed for the evaluation of the objective function were reported by Hajabdollahi et al. (2016). The parameters $\widehat{a}_c$ and $\widehat{b}_c$ for the evaluation of the capital cost are equal to 635.14 and 0.778, respectively. The energy price is 0.15 $/kWh, the pump efficiency is 0.6, the interest rate is 0.1 for a project horizon of 10 years, and the number of operating hours per year is 7500 h/y.

The optimization results for Area and *TAC* minimization are displayed in Table 5 and the corresponding global optimal solutions for each problem are depicted in Table 6.

The results displayed in Tables 5 and 6 illustrate a pattern of higher areas attained in *TAC* minimization compared to the Area minimization. This is expected because the total annualized cost seeks a trade-off between capital and operating cost, which is usually achieved by increasing the heat transfer area, i.e, with more plates and/or higher plate widths. In addition, the corrugation angles tend to be higher, because it reduces the flow turbulence and consequently the stream pressure drop. Finally, the solutions obtained by the TAC minimization may also seek heat exchangers with less number of passes, which is observed in Examples 1 and 4.

Tables 7 and 8 show the number of surviving candidates on each trimming and the number of candidates evaluated on the Smart Enumeration.

Tables 7 and 8 show that the Set Trimming eliminates on average

Table 7
Area minimization procedure.

		Example				
		1	2	3	4	5
Number of surviving candidates	Initial	79,000	79,000	79,000	79,000	79,000
	$\widehat{v_{min}} \leq v \leq \widehat{v_{max}}$	14,810	19,935	8,400	25,105	13,130
	$\Delta Ph \leq \Delta \widehat{Ph}_{disp}$	14,628	19,367	8,071	25,105	12,998
	$\Delta Pc \leq \Delta \widehat{Pc}_{disp}$	14,520	19,087	7,898	25,105	12,921
	$A \geq \widehat{A_{req}}$	14,339	15,152	4,098	25,105	8,833
Number of evaluations	Smart	819	2,064	1,355	898	3,164

Table 8
TAC minimization Procedure.

		Example				
		1	2	3	4	5
Number of surviving candidates	Initial	79,000	79,000	79,000	79,000	79,000
	$\widehat{v_{min}} \leq v \leq \widehat{v_{max}}$	14,810	19,935	8,400	25,105	13,130
	$A \geq \widehat{A_{req}}$	14,629	15,987	4,501	25,105	9,042
Number of evaluations	Smart	2,657	7,886	2,260	3,347	5,998

Table 9
Control parameters of the metaheuristic methods.

Method	Parameter
PSO	Number of particles = 100 Inertia weight = 0.5 Self-confidence factor = 1.5 Swarm confidence factor = 1.75
GA	Population size = 50 Crossover probability = 0.8 Mutation probability = 0.1 Elitism ratio = 0.02 Fraction of the population filled by members of the previous generation = 0.02 Crossover type = uniform

Table 10
Number of iterations of the metaheuristic methods.

	Example	GA	PSO
Area minimization	1	10	8
	2	25	15
	3	15	20
	4	20	8
	5	50	25
TAC minimization	1	40	15
	2	120	55
	3	30	8
	4	50	20
	5	70	30

almost 83% and 82% of the candidates for the Area and TAC minimization, respectively, which consumes a very small computational effort. In addition, the fraction of candidates evaluated in the Enumeration is on average only 2.1% and 5.6% of the original search space.

5.2. Comparison with other optimization methods

The PSO method was tested using the routine available in the module PySwarms (Miranda, 2018) using a rounding-off procedure to handle the discrete variables (Sengupta et al., 2018). The GA runs employed the module genetic algorithm (Solgi, 2020) according to Bozorg-Haddad et al. (2017). In all metaheuristic methods, the constraints were handled through the insertion into the objective function of penalty terms:

$$f = fobj + \sum_{i \in violatedconstraint} \left(\widehat{fobj}^{MAX} + 2\widehat{fobj}^{MAX} \Delta g_i \right) \tag{39}$$

where f is the objective function with the penalty term, $fobj$ is the original objective function (TAC or Area) calculated with Eq. (16) or Eq. (20), $\widehat{fobj}^{MAX}$ is the maximum value of the $fobj$ and Δg_i is the violation of the constraint i. In area minimization, $\widehat{fobj}^{MAX}$ corresponds to the largest area of the candidates. For the TAC minimization, $\widehat{fobj}^{MAX}$ is evaluated considering the largest area for evaluation of the capital costs and the largest pressure drop for the evaluation of the operating costs. Table 9 displays the set of control parameters employed in the runs of each stochastic method (Hajabdollahi et al., 2016).

Due to the randomized nature of the metaheuristic methods, they were tested through 5 independent runs. The number of iterations of each metaheuristic method was tuned through successive tests by increasing the number of iterations until the global optimum is identified in all runs or until the computational effort of the metaheuristic method becomes larger than the Partial Set Trimming followed by Smart Enumeration. Table 10 shows the corresponding number of iterations.

The area and TAC of the heat exchangers obtained using the metaheuristic methods are displayed in Tables 11 and 12, containing the best, worst, and average solution, and the percentage of the runs where the global optimum was found. Tables 12 and 13 present the elapsed time associated with each method. The values reported for the stochastic methods correspond to the average of the 5 runs.

Table 11, 12, 13 and 14 show that even with higher computational effort than the Smart Enumeration, the GA method got trapped in a local minimum on at least one run of all examples and formulations. For the PSO method, the results are similar, except for Example 4 in TAC minimization, where the method attained the global optimum in 100% of the runs with smaller elapsed times. Considering the general performance of the metaheuristic methods in all examples in both objective functions, the GA attained the global optimum in 14% of the runs and the PSO attained the global optimum in 34% of the runs. This result clearly illustrates the superiority of Smart Enumeration in this sample of examples, which always attain the global optimum.

Other important aspects need to be pointed out. The metaheuristic method attained poor local optima several times. For example, the PSO method did not find the global optimum in any of the 5 runs in Example 3, and the average values of the objective function are 23.5% and 14.2% higher than the global optimum in the area and TAC minimization,

Table 11
Optimization result for area minimization.

Example	Optimal area, m^2								This paper
	PSO				GA				
	Best	Average	Worse	% Global	Best	Average	Worse	% Global	Solution
1	91	96	111	40	91	113	128	20	91
2	199	224	312	20	205	299	351	0	199
3	148	168	187	0	187	218	258	0	136
4	122	132	155	40	126	139	150	0	122
5	200	222	236	40	200	252	334	20	200

Table 12
Optimization result for TAC minimization.

Example	Optimal TAC, $/y								This paper
	PSO				GA				
	Best	Average	Worse	% Global	Best	Average	Worse	% Global	Solution
1	10,782	11,435	13,917	40	10,782	11,188	12,578	20	10,782
2	17,149	17,641	17,969	40	17,149	17,651	18,005	40	17,149
3	8,372	9,549	10,207	0	9,724	10,255	10,785	0	8,364
4	25,250	25,250	25,250	100	25,250	25,442	25,696	20	25,250
5	14,816	15,636	15,841	20	14,816	15,829	16,192	20	14,816

Table 13
Elapsed time for area minimization.

Example	Elapsed time (s)		
	PSO	GA	This paper
1	251	157	93
2	492	474	323
3	584	201	140
4	378	395	124
5	743	747	398
Average	489.6	394.8	215.6

Table 14
Elapsed time for TAC minimization.

Example	Elapsed time (s)		
	PSO	GA	This paper
1	397	458	385
2	2,372	2,068	1,747
3	305	375	261
4	767	1,219	994
5	1,221	1,298	1,019
Average	1,012.4	1,083.6	881.2

Table 15
Global optimum solutions of the area minimization.

Approach	*Ntp*	Plate	*Nph*	*Npc*	β	Area (m^2)
Uniform physical properties	103	3	1	1	30	182
Variable physical properties	113	3	1	1	45	200

respectively. In addition, the result can be significantly dependent on the set of control parameters of the algorithms, different from the Smart Enumeration, which does not have any parameter to be tuned.

5.3. Effect of using uniform physical properties

The majority of previous papers about plate heat exchanger design optimization employed mathematical models that assume uniform physical properties. These models can provide satisfactory results in many problems, but if there is a considerable variation of the physical properties with temperature, the accuracy of the results can be compromised.

Aiming at illustrating the impact of the utilization of average values of the physical properties on the solution of the optimal design problem, we solved the area minimization problem for Example 5 considering uniform physical properties. The physical properties calculation method employed follows the procedure used by Incropera and Dewitt (2007), which uses the average temperature between the inlet and outlet design conditions for the evaluation of uniform physical properties.

Because the thermofluid-dynamic model uses a correction factor for evaluation of the convective heat transfer coefficient involving the viscosity calculated at the wall temperature, an iterative procedure is used for each candidate:

Step 1: Pick an initial estimate for the wall temperatures,
Step 2: Evaluate the viscosities at the wall condition,
Step 3: Evaluate the heat transfer coefficients,
Step 4: Simulate the heat exchanger,
Step 5: Return to Step 2 until the difference between the viscosities in successive iterations becomes smaller than a tolerance.

The optimization solutions using the uniform physical properties and physical properties evaluated locally are presented in Table 15.

The solution based on uniform physical properties attains an area 9% smaller than the proposed approach. Aiming to check the performance of this solution using rigorous modeling, the optimal heat exchanger obtained was simulated considering physical properties evaluated locally. The results are depicted in Table 16, together with the corresponding results obtained using uniform physical properties.

Table 16
Simulation results of the optimal solution with uniform physical properties.

Approach	Hot stream		Cold stream	
	Pressure drop (bar)	Outlet temperature (°C)	Pressure drop (bar)	Outlet temperature (°C)
Uniform physical properties	0.56	116.9	0.98	95.9
Variable physical properties	0.58	116.7	1.27	95.7

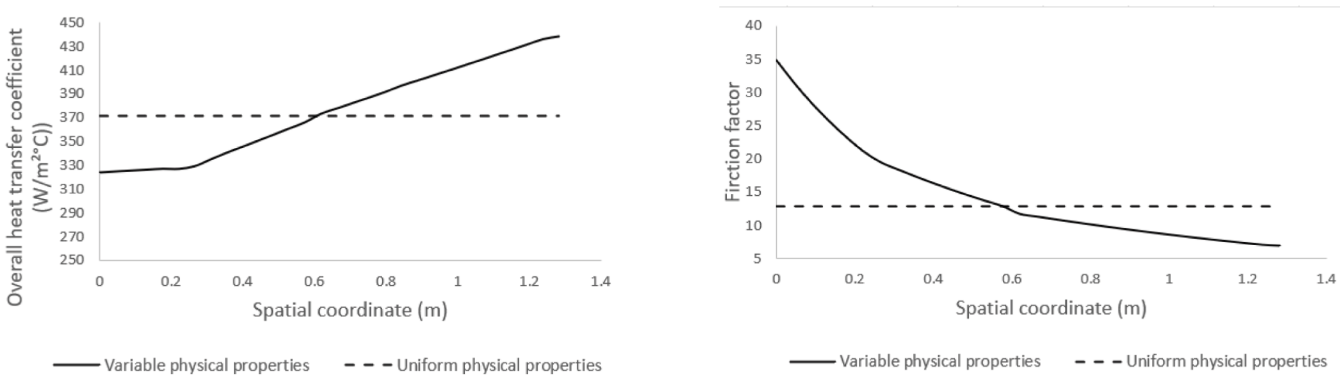

(a) Overall heat transfer coefficient profile

(b) Friction factor coefficient profile

Fig. 8. Properties profile.

Although both methods calculate similar outlet temperatures, the solution using physical properties calculated locally yields a higher cold stream pressure drop. Because the maximum pressure drop associated with the design task is limited to 1 bar, the more rigorous simulation results using variable physical properties indicate that this design solution is not feasible.

Fig. 8 depicts the overall heat transfer coefficient and the friction factor profiles through one of the channels (channel #56). These profiles illustrate why the thermal results using uniform properties were similar to those using variable properties, but the hydraulic results are considerably different.

Despite the significant variation of the overall heat transfer coefficient along the channel (328 W/(m$^{2\circ}$C) – 450 W/(m$^{2\circ}$C)), the simulation using uniform properties achieves a good representative value 371 W/(m$^{2\circ}$C), which is only 0.9% smaller than the average value of the corresponding results of the rigorous model. However, the simulation using uniform properties renders a friction factor 12.2% smaller than the average value using the rigorous model, which explains the large cold stream pressure drop difference.

6. Conclusions

This paper presented the solution for the optimal design of gasketed plate heat exchangers. We improve upon the models and solution procedures proposed in the literature. We address a differential model that takes into account different arrangements of passes, we employ a rigorous model that considers the variation of the physical properties with temperature and end plate effects. We introduce the use of a new optimization approach, based on Partial Set Trimming followed by Smart Enumeration. Proxy set trimming is used. This variant of the Set Trimming technique was not proposed originally (Costa and Bagajewicz, 2019). Partial Set trimming followed by Smart Enumeration has several advantages that overcome important limitations observed in previous attempts to solve the design problem using MINLP procedures: it always attains the global optimum, it does not present convergence limitations, and its performance does not depend on any parameter tuning. In addition, although we use finite differences and solve a system of equations in this paper, the technique has the potential to avoid embedding complex finite difference equations into the mathematical model and allows the use of any ODE integrator (Runge Kutta, LSODE), which improves the accuracy of the results. Finally, based on a sample of five different design examples, the proposed approach presented a better performance than two metaheuristic methods.

Declaration of Competing Interest

The authors declare that they have no known competing financial interests or personal relationships that could have appeared to influence the work reported in this paper.

Data availability

No data was used for the research described in the article.

Acknowledgments

André L. M. Nahes thanks the Coordination for the Improvement of Higher Education Personnel (CAPES) for his scholarship. André L. H. Costa would like to thank the National Council for Scientific and Technological Development (CNPq) for the research productivity fellowship (Process 310390/2019-2) and the Rio de Janeiro State University through the Prociência Program. Miguel Bagajewicz thanks the visiting researcher scholarship from UERJ (PAPD Program) for part of the time of the development of this work.

References

O. Bozorg-Haddad M. Solgi H.A. Loáiciga Meta-Heuristic and Evolutionary Algorithms for Engineering Optimization 1 2017 Wiley.
Cao, E., 2010. Heat Transfer in Process Engineering. McGraw-Hill, New York.
Costa, A.L.H., Bagajewicz, M.J., 2019. 110th Anniversary: on the departure from heuristics and simplified models toward globally optimal design of process equipment. Ind. Eng. Chem. Res. 58, 18684–18702.
Daichendt, M.M., Grossmann, I.E., 1994. Preliminary screening procedure for the MINLP synthesis of process system-II. Heat exchanger networks. Comput. Chem. Eng. 679–709.
Goldberg, D.D., 1989. Genetic Algorithms in Search, Optimization, and Machine Learning. Addison-Wesley Professional.
Guo-Yan, Z., En, W., Shan-Tung, T., 2008. Techno-economic study on compact heat exchangers. Int. J. Energy Res. 32, 1119–1127.
Gut, J.A.W., Pinto, J.M., 2004. Optimal configuration design for plate heat exchangers. Int. J. Heat Mass Transf. 47, 4833–4848.
Hajabdollahi, F., Hajabdollahi, Z., Hajabdollahi, H., 2013. Optimum design of gasket plate heat exchanger using multimodal genetic algorithm. Heat Transfer Res. 44, 761–789.
Hajabdollahi, H., Naderi, M., Adimi, S., 2016. A comparative study on the shell and tube and gasket-plate heat exchangers: the economic viewpoint. Appl. Therm. Eng. 92, 271–282.
Imran, M., Pambudi, N.A., Farooq, M., 2017. Thermal and hydraulic optimization of plate heat exchanger using multi objective genetic algorithm. Case Stud. Therm. Eng. 10, 570–578.
Incropera, F.P., Dewitt, D.P., 2007. Fundamentals of heat and mass transfer. John Wiley & Sons, New York.
Kakac, S., Liu, H., 2002. Heat Exchangers: Selection, Rating, and Thermal Design, 2nd ed.;. CRC Press, Boca Raton, pp. 373–412.
J. Kennedy, R. Eberhart, Particle Swarm Optimization. International Conference on Neural Networks, 1995.

N.R. Martins, P. Cheali, A.L.H. Costa, M.J. Bagajewicz, In Global Optimization of Counter Current Gasketed Plate Heat Exchanger, Proceedings of the 29th European Symposium on Computer Aided Process Engineering, Eindhoven, Netherlands, June 16–19, 2019.

Miranda, L.J., 2018. PySwarms: a research toolkit for particle swarm optimization in python. Journal Open Source Software.

Mota, F.A.S., Ravagnani, M.A.S.S., Carvalho, E.P.M., 2014. Optimal design of plate heat exchangers. Appl. Therm. Eng. 63, 33–39.

Nahes, A.L.M., Martins, N.R., Bagajewicz, M.J., Costa, A.L.H., 2021. Computational study of the use of set trimming for the globally optimal design of gasketed-plate heat exchangers. Ind. Eng. Chem. Res. 60 (4), 1746–1755.

Nahes, A.L.M., Bagajewicz, M.J., Costa, A.L.H., 2022. Simulation of gasketed-plate heat exchangers using a generalized model with variable physical properties. Appl. Therm. Eng. 217, 119197.

Najafi, H., Najafi, B., 2010. Multi-objective optimization of a plate and frame heat exchanger via genetic algorithm. Heat Mass Transf. 46, 639–647.

Picón-Núñez, M., Polley, G.T., Jantes-Jaramillo, D., 2010. Alternative design approach for plate and frame heat exchangers using parameter plots. Heat Transfer Eng. 31 (9), 742–749.

Raja, B.D., Jhala, R.L., Patel, V., 2018. Thermal-hydraulic optimization of plate heat exchanger: a multi-objective approach. Int. J. Therm. Sci. 124, 522–535.

Saleh, K., Aute, V., Radermacher, R., Azarm, S., 2013. Chevron plate heat exchanger optimization using efficient approximation-assisted multi-objective optimization techniques. HVAC&R Res. 19, 788–799.

Saunders, E.A.D., 1988. Heat Exchangers: Selection, Design, and Construction. John Wiley & Sons, New York.

Sengupta, S., Basak, S., Peters II, R.A., 2018. Particle Swarm Optimization: a Survey of historical and recent developments with hybridization perspectives. Mach. learn. knowl. extr. 1, 157–191.

Shah, R.K., Sekulic, D.P., 2003. Fundamentals of Heat Exchanger Design. John Wiley & Sons, Hoboken.

Shokouhmand, H., Hasanpour, M., 2020. Effect of flow maldistribution on the optimal design of plate heat exchanger using constrained multi objective genetic algorithm. Case Stud. Therm. Eng. 18, 100570.

M. Solgi, Genetic algorithm 1.0.1, 2020.

Towler, G., Sinnot, R., 2008. Chemical Engineering Design – Principles. Practice and Economics of Plant and Process Design, Butteworth-Heinemann, Burlington.

Wang, L., Sundén, B., 2003. Optimal design of plate heat exchangers with and without pressure drop specifications. Appl. Therm. Eng. 23, 295–311.

Xu, K., Qin, K., Wu, W., Smith, R., 2022. A new computer-aided optimization-based method for the design of single multi-pass plate heat exchangers. Processes. 10, 767.

Zhu, J., Zhang, W., 2004. Optimization design of plate heat exchangers (PHE) for geothermal district heating systems. Geothermics 33 (3), 337–347.